Numerical Expansion Analyses of the Strategic Petroleum Reserve in Bayou Choctaw Salt Dome, USA

B.Y. Park & C.G. Herrick
Sandia National Laboratories, Carlsbad, NM, U.S.A.

B.L. Ehgartner
Sandia National Laboratories, Albuquerque, NM, U.S.A.

ABSTRACT: This paper develops a series of three-dimensional simulations for the Bayou Choctaw Strategic Petroleum Reserve. The U.S. Department of Energy plans to leach two new caverns and convert of one of the existing caverns within the Bayou Choctaw salt dome to expand its petroleum reserve storage capacity. An existing finite element mesh from previous analyses is modified by adding two caverns and increasing the size of existing Cavern 102. The structural integrity of the three expansion caverns and the interaction between all the caverns in the dome are investigated. The impacts of the expansion on underground creep closure, surface subsidence, infrastructure stability, and well integrity are quantified. The results show that from a structural viewpoint, the locations of the two newly proposed expansion caverns are acceptable, and all three expansion caverns can be safely constructed and operated.

1 INTROUCTION

The Strategic Petroleum Reserve (SPR) currently stores over 700 million barrels (MMB) of crude oil at four sites located along the Gulf Coast. The capacity of the existing 62 caverns is 727 MMB. The U.S. Department of Energy (DOE) decided to increase the size of the reserve to 1 billion barrels. While this will require the development of a new site, existing sites will be enlarged. At Bayou Choctaw (BC), the current storage capacity of 76 MMB will be expanded to 109 MMB through the leaching of two new 11.5 MMB caverns and acquisition of one existing 10 MMB cavern.

This paper develops a series of three-dimensional structural simulations of BC SPR salt dome. In a previous paper, Park et al. [2008] developed a three-dimensional FEM analysis to model the caverns in the dome. Fifteen active and nine abandoned caverns exist currently at BC, with a total cavern volume of some 164 MMB. The DOE has a plan to leach two additional caverns and convert one extant cavern within the BC salt dome [URS, 2006]. Ehgartner and Lord [2006] suggested the location for two new caverns at BC. Cavern 102, a former Union Texas Petroleum (UTP) cavern, is potentially available for conversion to a SPR cavern. The DOE would like to acquire it as part of the expansion. This paper attempts to investigate the structural integrity of the three expansion caverns and their interaction with other caverns in the dome. The impacts of the expansion by three caverns on underground creep closure, surface subsidence, infrastructure, and well integrity are quantified.

2 ANALYSIS MODEL

2.1 *Geomechanical Model*

Salt dome geometry
The stratigraphy near the BC salt dome is shown in Figure 1 (left). The top layer is overburden, which consists of sand, silts and clays and has a thickness of approximately 152 m. Below the overburden is the caprock, which consists of gypsum, anhydrite, and sand and is about 46 m thick. The bottom boundary of the analyses, which is considered the depth of the salt dome, is set at 2438 m below the surface. All SPR caverns are located below 610 m from the surface.

Figure 1 (right) shows a vertical cross-section of the BC site. The horizontal shape of the dome is approximately elliptical. The major and minor radii are measure 1488 m and 1300 m, respectively. The caverns planned for expansion are drawn in blue.

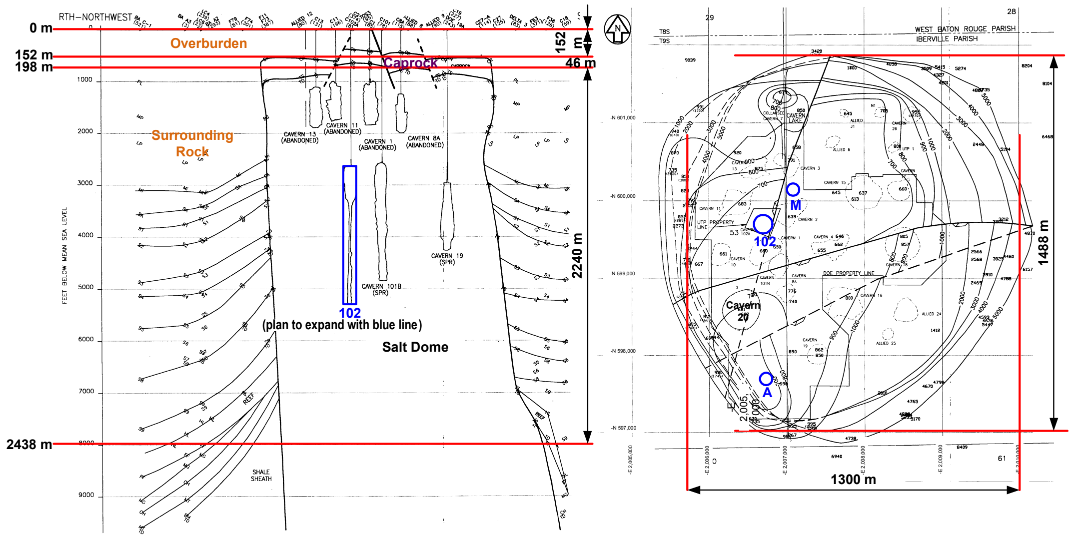

Figure 1. Stratigraphy (left) and plan view (right) at 1219 m BMSL* near the Bayou Choctaw salt dome [Neal et al., 1993]. The caverns drawn in blue line indicate the proposed two new caverns (A and M) and cavern to be converted (102).

Salt constitutive model

A power law creep model is used for the salt creep constitutive model, which considers only secondary or steady-state creep. The creep strain rate is given by:

$$\dot{\varepsilon} = A\left(\frac{\sigma}{\mu}\right)^n \exp\left(-\frac{Q}{RT}\right) \tag{1}$$

where, $\dot{\varepsilon} =$ secondary creep strain rate; $\sigma =$ von Mises equivalent stress (Pa); $\mu =$ elastic shear modulus = $E/2(1+\nu)$ (Pa); $E =$ elastic modulus (Pa); $\nu =$ Poisson's ratio; T = absolute temperature (K); A = structure factor determined from fitting the model to creep data, n = stress exponent; Q = effective activation energy (cal/mole); and R = universal gas constant (cal/(mole·K)).

The geomechanical properties of BC salt are not known entirely for modeling. The field data for the structure factor, the stress exponent, and the thermal constant have not been determined. The values of the stress exponent and the thermal constant are assumed to be the same as the values obtained from WIPP rock salt. The structure factor was determined by Park et al. [2006] through a number of back-fitting analyses. The values used as input data in the present analyses are listed in Table 1.

Lithologies around the salt dome

An elastic model is assumed for the lithologies encompassing the salt dome. The surface overburden layer, which is mostly comprised of sand, is assumed to exhibit elastic material behavior. The sand layer is considered isotropic, and has no assumed failure criteria. The required model parameters for the overburden are not available for BC, so the McCormick Ranch Sand properties used in the West Hackberry analysis [Ehgartner and Sobolik, 2002] were used. The caprock layer, consisting of gypsum, anhydrite and sand, is also assumed to behave elastically. Samples of caprock from two different core holes at BC were tested by Dames and Moore [1978] to determine physical properties. The tested samples were from massive gypsum-anhydrite units at

* Below Mean Sea Level

depths of 183 m and 197 - 198 m in Core Hole 1 and 170 - 196 m in Core Hole 2 [Hogan, 1980]. The rock surrounding the salt dome is a sedimentary rock that consists mostly of sandstone and shale. It is assumed to be isotropic, homogeneous elastic rock. The required model parameters of the surrounding rocks are also not available. Typical values for the Young's moduli of sandstones and shales range from 0.4 to 69 GPa [Carmichael, 1984]. For simplifying the back-fitting analysis, a median value for the Young's modulus of sandstone, 35 GPa, is assumed. The mechanical properties used in the present analysis are listed in Table 2.

Table 1. Material properties of Bayou Choctaw salt used in the analyses.

Parameter	*Unit*	*Value*	*Reference*
Young's modulus (E)	GPa	31	[Krieg, 1984]
Density (ρ)	kg/m^3	2300	[Krieg, 1984]
Poisson's ratio (ν)	-	0.25	[Krieg, 1984]
Elastic modulus reduction factor (RF)	-	12.5	[Morgan and Krieg, 1988]
Bulk modulus (K)	GPa	1.653	Calculated using E and ν
Two mu (2μ)	GPa	1.984	Calculated using E and ν
Structure multiplication factor (SMF)	-	0.12	[Park et al., 2006]
Calibrated structure factor (A)	$Pa^{-4.9}/s$	6.95×10^{-37}	[Park et al., 2006]
Stress exponent (n)	-	4.9	[Krieg, 1984]
Activation energy (Q)	cal/mol	12000	[Krieg, 1984]
Universal gas constant (R)	cal/(mol·K)	1.987	-
Input thermal constant (Q/R)	K	6039	-

Table 2. Material properties of lithologies around salt dome used in the analyses.

	Unit	*Overburden*	*Caprock*	*Surrounding Rock*
Young's modulus	GPa	0.1	15.7	35
Density	kg/m^3	1874	2319	2500
Poisson's ratio	-	0.33	0.288	0.33

2.2 *Cavern Model*

Cavern geometry and layout

The cavern shapes and locations vary widely as shown in Figure 1. Since the three caverns planned for the expansion, the six existing SPR caverns, and seventeen other caverns have structural interactions, a model including all caverns in the dome was used to investigate the structural behavior.

Caverns A and M are planned to have the same size and will be leached at the same elevation. Their height will be 610 m with a roof elevation of -762 m. The roof and floor diameters for the bifrustum shape are 33.5 m and the middle diameter is 91.4 m. The diameters enlarge up to 50.3 m at both ends and 129.8 m in the middle, respectively, after five drawdowns†. Design criteria for DOE caverns is governed by a requirements document [DOE, 2001]. Cavern 102, the converted UTP cavern, will have a height of 823 m from its original elevation (the roof elevation is -805 m) and an initial diameter of 76.2 m. The diameter enlarges up to 108.2 m after five drawdowns. The DOE plans on leaching the existing cavern to create enough volume to accommodate an additional 10 MMB of storage.

Model history

The drill dates of the existing caverns varied from 1934 to 1990. The last sonar measurements to determine the cavern shapes were taken between 1977 and 1993 [Hogan, 1980; Neal et al., 1993]. For the purposes of the present simulation and to simplify the model history, it is assumed that the initial leaching of all existing caverns began 21 years ago in 1987. This is consi-

† "Drawdown" is when the crude oil is withdrawn from the cavern. Fresh water is used to withdrawal the crude oil. Because the cavern enlarges due to salt dissolving from the cavern walls, it is called a "drawdown leach".

dered time t = 0 years. After that, leaching to expand Cavern 102 will start at 21 years and will be completed one year later at 22 years. The initial leaching of Caverns A and M will start at 22 years and 23 years, respectively, with leaching continuing for one year. Figure 2 shows the time sequence of the initial cavern leaches, the expansion leaches, and five drawdown leach times used in the simulation.

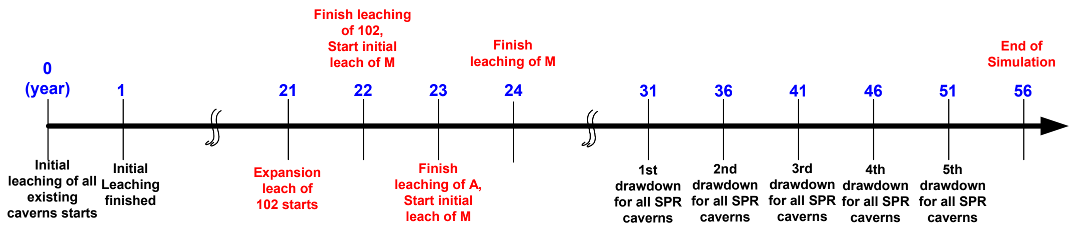

Figure 2: The time sequence for the simulation.

The analysis simulates caverns that were leached to full size over a one year period by means of gradually switching from salt to fresh water in the caverns. It was assumed that the SPR caverns were filled with petroleum and non-SPR caverns were filled with brine at year one after the initial leach starts. The existing caverns are simulated as undergoing creep for thirty years. The expansion SPR Cavern 102 is permitted to creep for nine years after completion of expansion leaching in year 22. The new SPR Caverns A and M are permitted to creep for eight and seven years, respectively, after their initial leaching cycles are completed in years 23 and 24, respectively. The simulation will then perform oil drawdowns in the SPR caverns.

Every 5 years after the thirty-first year of the simulation, every SPR cavern is modeled as being instantaneously leached. Modeling of the drawdown process of the caverns was performed by deleting elements along the walls of the caverns so that the volume increased by 15% with each leach. Leaching is assumed to occur uniformly along the entire height of the cavern. However, leaching is not permitted in the floor or roof of the caverns. The 5-year period between each drawdown allows the stress state in the salt to return to a steady-state condition, as will be evidenced in the predicted closure rates. The simulation was continued until after the 5th drawdown to investigate the structural behavior of the dome for a total of 56 years. Creep closure is allowed to occur in all caverns during the simulation period.

The pressure conditions applied to the caverns are based on average wellhead pressures. For example, Cavern 15 is operated over a range of pressures from 5.6 to 6.8 MPa under normal conditions. The pressure starts at 5.6 MPa, then, due to creep closure and thermal expansion of the fluids, the pressure gradually rises to 6.8 MPa. At that time the brine is removed from the cavern to reduce the pressure down to 5.6 MPa again. Thus, on average, a pressure of 6.2 MPa is used for Cavern 15 as the operating wellhead pressure under normal conditions. In the same manner, the pressures of 6.2, 4.9, 6.4, 5.9, and 6.3 MPa are used for the normal operating wellhead pressures of Caverns 17, 18, 19, 20, and 101, respectively [Park et al., 2008]. It is assumed that the normal operating wellhead pressures of caverns for the expansion 102, A, and M, are the same as that of Cavern 101 because the casing seat depths of the caverns will all be approximately the same.

In general, the SPR caverns are most likely to become structurally unstable when a workover[‡] is in progress. In this analysis, the workover is simulated by means of an internal pressure change in the SPR caverns. The following workover processes are used to investigate the structural stability of the caverns:

- A constant pressure is applied for the majority of the time, with pressure drops periodically included.
- For workover conditions, zero wellhead pressure is used.

‡ "Workover" is when the wellhead pressure in the cavern is dropped to zero for maintenance.

- Caverns 15 and 17 are worked over together one year after switching from brine to petroleum. After that, workovers are performed on Caverns 102, 19, and 18 in order. Then, after 2.2 more years, Caverns 20, 101, A, and M, respectively, are worked over one by one
- Workover durations are 1 month for all caverns, because the workover durations for the existing caverns varied from 22 days to 36 days.
- This workover cycle is repeated every 5 years.
- For both normal and workover conditions, the caverns are assumed to be full of oil having a pressure gradient of 8370 Pa/m of depth.
- The pressure due to the oil head plus the wellhead is applied on the cavern boundary during the normal operation.

For the non-SPR caverns, except Cavern 7, a pressure due to brine head and pressure gradient of 11,763 Pa/m is applied on the cavern boundaries. In case of Cavern 7, a pressure gradient of 9048 Pa/m is applied on the wall and 18,368 Pa/m is applied on the floor and roof in order to represent the collapsed state of the cavern [Park et al., 2008].

Thermal conditions

The finite element model includes a depth-dependent temperature gradient which starts at 28.90°C at the surface and increases at the rate of 0.0251°C/m. The temperature profile is based on the average temperature data recorded in well logs from BC prior to leaching [Ballard and Ehgartner, 2000]. The temperature distribution is important because the creep response of the salt is temperature dependent. Radial temperature gradients due to cavern cooling effects from the cavern contents are not considered in these calculations. Previous 2D cavern studies have shown the predicted cavern deformation to be insensitive to the developed radial thermal gradients [Hoffman, 1992].

3 MESH GENERATION

Two new caverns, A and M, and the conversion of Cavern 102 were added into the existing mesh used for previous analyses [Park et al., 2008]. Figure 3 shows an overview of the finite element meshes of the stratigraphy and cavern field at BC. The shapes of Caverns A and M are modeled as bifrustum while Cavern 102 is modeled as a cylinder. The meshes have been separated to show the individual material blocks. The X-axis of model is in the EW direction, Y-axis is in the NS direction, and Z-axis is the vertical direction. Four material blocks are used in the model for the overburden, caprock, salt dome, and surrounding rocks. The six existing SPR, three expansion SPR, two inactive, seven abandoned, and eight UTP caverns are modeled within the salt dome mesh. The hands point to the locations of the two new caverns and the converted cavern.

Figure 4 shows the assembled mesh and the boundary conditions used for the modified BC model. The salt dome is modeled as having fixed far-field boundary conditions. The lengths of the confining boundaries are 7440 m in the NS direction and 6500 m in the EW direction. These lengths are about five times the major or minor diameter of the salt dome, respectively. This ratio (5) is far better than the generally accepted ratio (3 to 4) between the maximum dimensions/minimum excavation sizes. The mesh consists of 777,665 nodes and 762,636 elements. The models consist of 13 element blocks, 73 side sets, and 6 node sets.

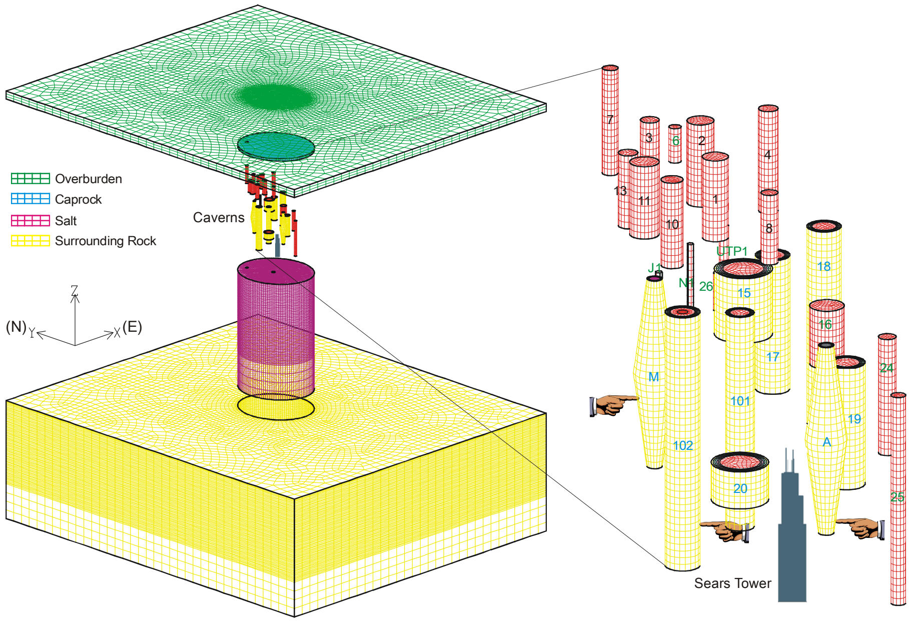

Figure 3. Overview of the finite element mesh of the stratigraphy and cavern field at Bayou Choctaw and the cavern geometry within the salt dome. The hands are pointing to caverns for the expansion. For comparison purposes to show how large the caverns are, a silhouette of the Sears Tower is shown.

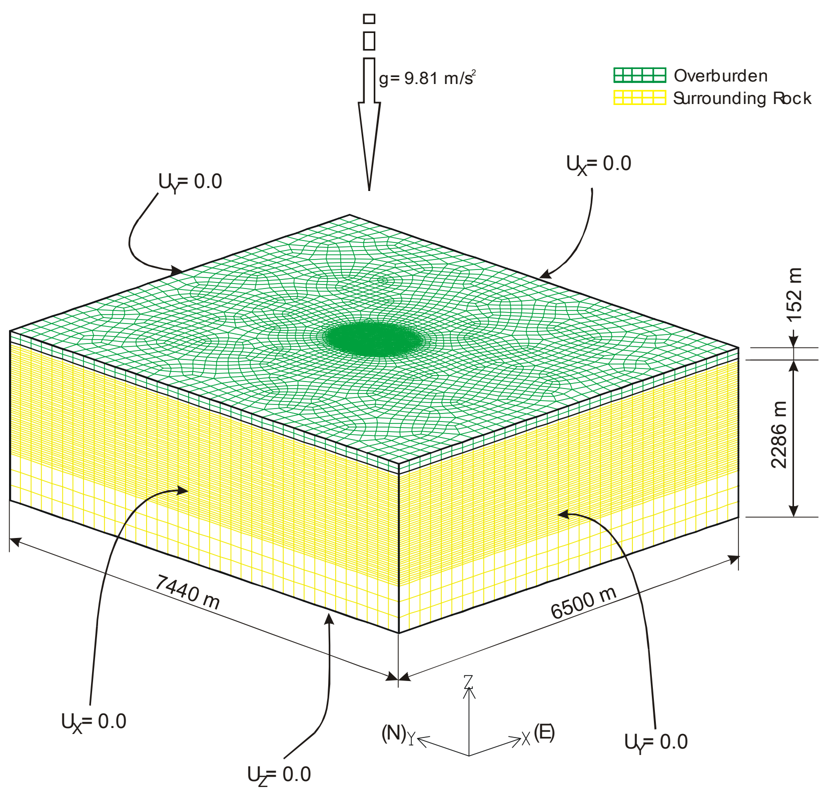

Figure 4. Finite mesh discretization and boundary conditions at Bayou Choctaw.

4 FAILURE CRITERIA

4.1 *Structural Stability of Salt Dome*

Potential damage to or around the new and converted SPR caverns was evaluated based on two failure criteria: dilatant damage and tensile failure.

To check for dilatant damage, the dilatancy criterion discussed in the previous analyses [Park et al., 2008] is used.

$$D = \frac{0.257 \cdot I_1}{\sqrt{J_2}} \tag{1}$$

where, $D =$ damage factor

$I_1 = \sigma_1 + \sigma_2 + \sigma_3 = 3\sigma_m$: the first invariant of the stress tensor.

$\sqrt{J_2} = \sqrt{\dfrac{(\sigma_1 - \sigma_2)^2 + (\sigma_2 - \sigma_3)^2 + (\sigma_3 - \sigma_1)^2}{6}}$: the square root of the second invariant of the deviatoric stress tensor

σ_1, σ_2, and σ_3 are the maximum, intermediate, and minimum principal stresses, respectively. σ_m is the mean stress.

When $D \le 1$, the shear stresses in the salt (J_2) are large compared to the mean stress (I_1) and dilatant behavior is expected. When $D > 1$, the shear stresses are small compared to the mean stress and dilatancy is not expected. The stability of the caverns may be controlled by weaker dirty salts and the variability in the measured strength and dilatancy values, so a 20% uncertainty in the safety factor is used with this criterion. Therefore an allowable safety factor against dilatancy is assumed to be 1.2 in this study.

In addition, in order to check for possible tensile failure of the salt, the tensile strength is conservatively assumed to be zero. Tensile cracking in rock salt initiates perpendicular to the largest tensile stress direction.

4.2 *Allowable Strains for Well and Surface Structures*

The physical presence of wells and surface structures are not modeled in the finite element analysis, but the potential for ground deformation producing damage in these structures can be conservatively estimated by assuming that they will deform according to the predicted ground deformation.

Subsidence will primarily induce elongation of the axis of the well. Under these conditions, the cemented annulus of the wells may crack, forming a horizontal tensile fracture that may extend around the wellbore. Vertical fluid migration is not expected under these conditions, however horizontal flow could occur. The allowable axial strain for purposes of this study is assumed to be 2 millistrains in compression and 0.2 millistrains in tension [Thorton and Lew, 1983]. The benefit of the steel casings in reinforcing the strength of the cement, especially under elongation, is not accounted for in this evaluation. The 2 millistrain limit is also representative of the typical yield point for steel casings in the SPR.

Structural damage on the surface is typically caused by the accumulation of large surface strains due to subsidence. These strains can cause distortion, damage, and failure of infrastructure such as buildings, pipelines, roads, and bridges. Surface strains will accumulate in structures over time, which increases the possibility of damage in older facilities. For purposes of this study, the allowable strain is taken to be 1 millistrain for both compression and tension.

5 ANALYSIS RESULTS

5.1 *Storage Loss*

Figure 5 show the predicted total volumetric closure normalized to overall storage volume for the current six SPR caverns before expansion starts at 21 years, then for the six SPR caverns and the three additional SPR caverns after expansion is completed at 24 years. Because the current set of caverns are initially leached at the beginning of the analysis, the expansion cavern leaches are completed at 24 years, and then the leaching cycle begins at 31 years and occurs every 5 years thereafter, the percentage of closure is normalized by the cavern volume immediately following each leach. The rates of decrease are about 1.5% at 21 years. These rates are the same as the results from the previous analyses [Park et al., 2008] because the expansion does not start in the present model until 21 years. The impact of workover pressure is also evident in Figure 5 by the abrupt change in normalized volumetric closures that occur each month following leach.

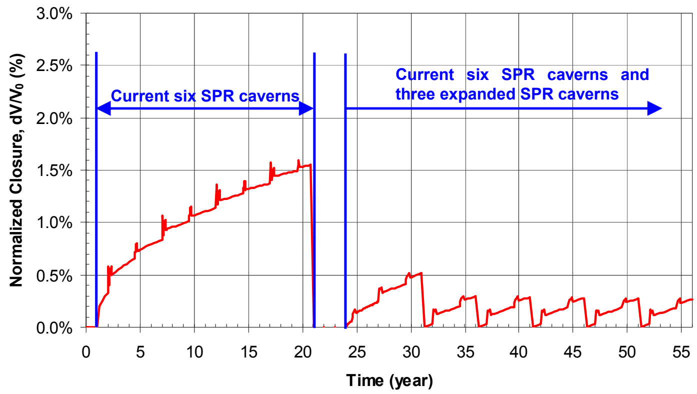

Figure 5. Predicted total volumetric closure normalized to overall storage volume.

5.2 *Subsidence*

Figure 6 show the calculated surface strains at 21 years before inclusion of any additional caverns and 56 years after 5th drawdown of the expanded cavern field. At both times, the accumulated strain is below the limiting value of 1 millistrain and thus structural damage should not occur. There is no marked increase in surface strains due to the expansion at 21 years.

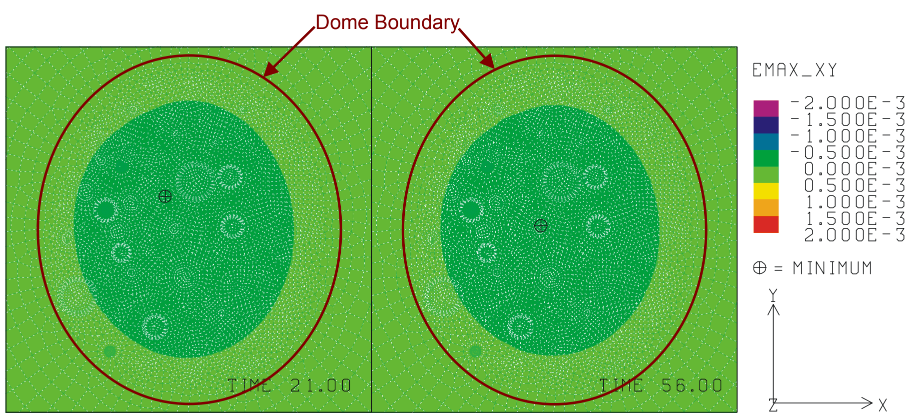

Figure 6. Predicted radial surface strains at 21 years and 56 years.

5.3 *Cavern Wells*

The calculated vertical ground strains around the expansion caverns are shown in Figure 7 at 31 years (prior to 1st drawdown) and 56 years (after the 5th drawdown). Of interest are the strain magnitudes in the proximity of the cavern wells from the surface to the cavern roofs. Well casings typically extend from the surface to about 30 m above the cavern roof. The collapse strength of the steel component of a well is reduced as the casing stretches. In general, steel casing will not yield until about 2 millistrain. Also, fracturing in the grout surrounding the steel is thought to occur for tensile strains greater than 0.2 millistrain. Therefore, predicted strains near the cavern wells larger than 0.2 millistrain in tension are predicted to cause failure in the grout.

The predicted strains over 30 m above the cavern roofs of Caverns A, M, and 102 at 31 and 56 years are less than 2 millistrains, thus the steel casing should not yield. The vertical lines in the plots are the edges of the model elements.

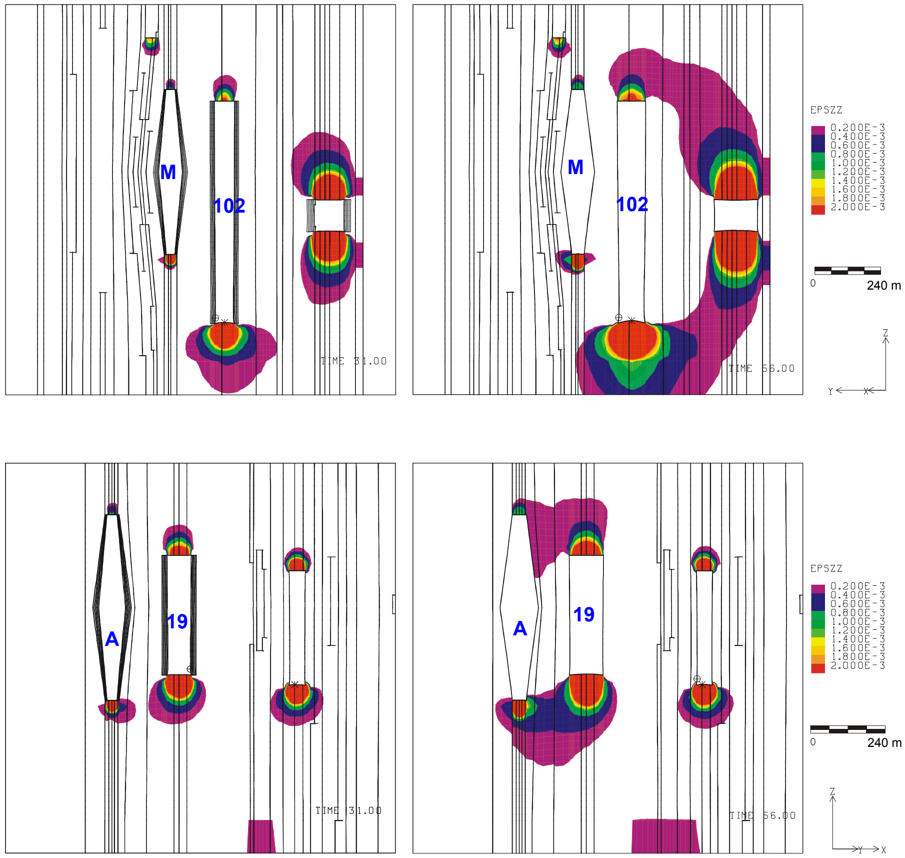

Figure 7. Vertical strains around cylindrical Cavern 102 and bifrustum-shaped Caverns M and A prior to 1st leach (left) and after the 5th leach (right). Positive indicates tensile strain.

5.4 *Cavern Stability*

Minimum compressive stress

Figure 8 shows the predicted minimum compressive stress[§] (MCS) histories for the salt dome and for only the caverns below 610 m. The MCS in the entire salt dome is calculated as -2.07 MPa at 1 year when the brine in the SPR caverns was switched to oil. Note that the negative sign (-) indicates a compressive stress and the positive sign (+) indicates a tensile stress. All stresses around the caverns at all times were found to be compressive (less than 0 Pa). Thus, all caverns are structurally stable against tensile failure throughout the entire simulation time because the potential for tensile failure exists only if the MCS is numerically zero or is positive (i.e. tensile) as mention in Section 4.1. The most critical location in the salt dome was found to be in the top of the dome because of earth pressure. The compressive stress increases with depth. Having the MCS on the top of the dome is not of interest because all SPR caverns are located below 610 m. The data for ‘Below 610 m’ in Figure 8 means that the data above 610 m is screened out to show the detailed change of MCS around the SPR caverns.

[§] Compressive stresses are calculated in every element in the salt dome at each time step. The minimum compressive stress means the minimum value among the stresses in every element at a specific time.

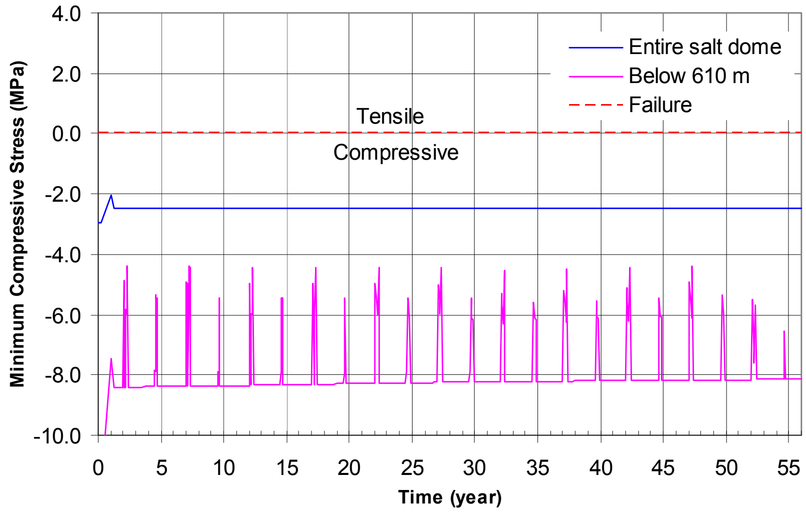

Figure 8. Predicted minimum compressive stress history in the salt dome.

Minimum safety factor against dilatant damage

The minimum safety factor** histories against dilatancy damage (DILFAC) is plotted in Figure 9. The DILFAC is predicted to be 1.2 at 47.08 years. The potential dilatant failure occurs since the DILFAC is 1.2 or less as discussed in Section 4.1.

To examine the location where the failure may occur in the salt dome, DILFAC histories in the elements within 40 m of Cavern 15, 17, 102, A, and M are plotted in Figure 10. A DILFAC of 1.2 is predicted around Caverns 15 and 17 at 47.08 years when the workover on the Caverns 15 and 17 is performed after the fourth leach (Figure 10 (a)). The web of salt between Caverns 15 and 17 has the lowest predicted safety factor of the caverns in the dome. This is similar to the results obtained in previous analyses [Park et al., 2008].

The DILFACs at 2.03 years, 22.17 years, 24.75 years and 24.83 years are predicted to be closer to 1.2 than at other times in Figure 9. These are the times of the first workovers after the initial leach. The first workover after the expansion leach of Cavern 102 is performed at 22.17 years. The lowest safety factor for Cavern 102 is predicted at the time of the first workover after the expansion leach (Figure 10 (b)). The weakest spot against dilatant damage appears around Cavern 102, but not in the vicinity of Cavern 15 and 17 at this time. This suggests that the first workover after the expansion of Cavern 102 needs to be performed more carefully than other workovers. In the same manner, the lowest safety factors for Caverns A and M are predicted during the first workovers after their initial leaches as shown Figure 10 (c) and (d), respectively.

All safety factors in the elements within 40 m of Caverns M, 102, and A were found to be larger than 1.2. Thus, Caverns A, M, and 102 appear to be structurally stable against dilatant damage throughout the entire simulation time. This suggests that Caverns A and M can be safely leached and Cavern 102 can be safely converted in the BC salt dome. The planned locations of Caverns A and M are found to have no problem from a structural stability viewpoint according to this analysis.

** The safety factors are calculated in every element in the salt dome at each time step. The minimum safety factor means the minimum value among the safety factors in every element at a specific time.

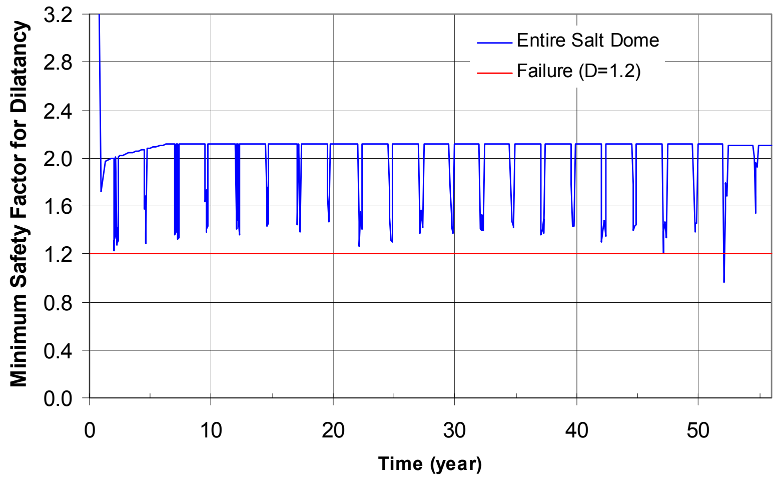

Figure 9. Minimum safety factor history against dilatant damage.

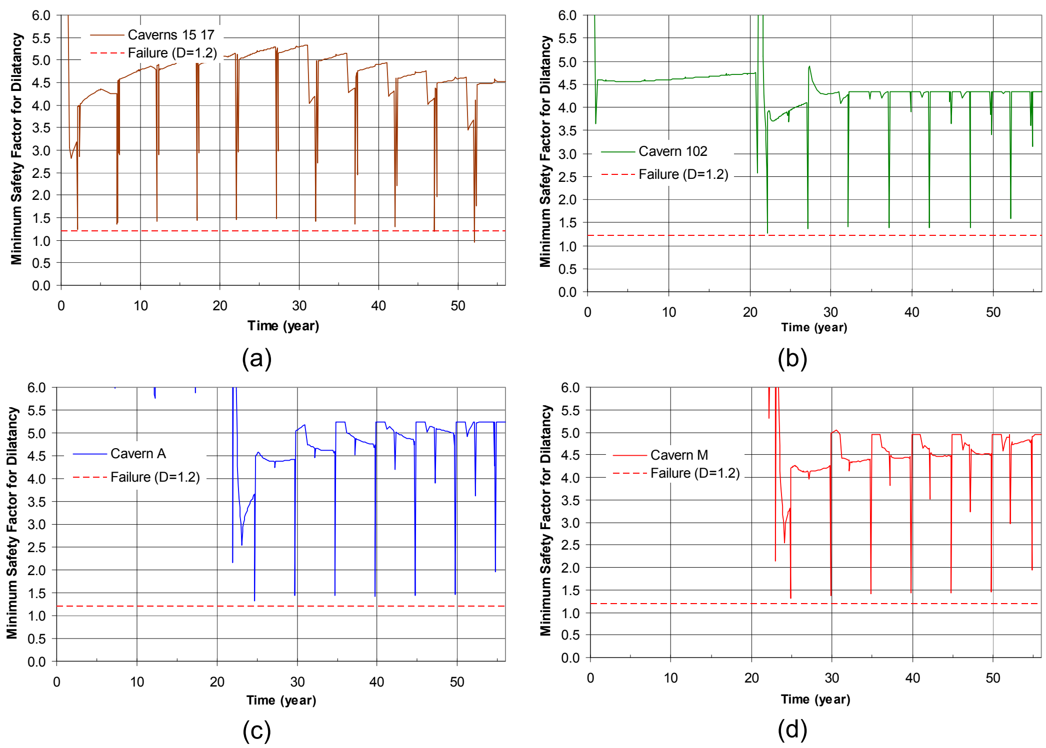

Figure 10. Minimum safety factor history against dilatant damage in the elements within 40 m of Caverns 15 and 17 (a), 102 (b), A (c) and M (d).

6 SUMMARY AND CONCLUDING REMARKS

An existing three dimensional FEM mesh from a previous analyses was modified to include the addition of two new caverns and conversion of another for SPR purposes. The structural stability for the BC dome was evaluated based on the failure criteria for dilatant damage and tensile failure. The impacts of the expansion of three caverns on underground creep closure, surface subsidence, infrastructure, and well integrity were investigated.

The additional three SPR caverns considered for expansion along with the extant caverns in the dome are predicted to be structurally stable against tensile failure. Dilatant failure is not expected to occur within the vicinity of the three expansion caverns. Damage to surface structures was not predicted because there was not a predicted marked increase in surface strains due to the addition of the three caverns. The predicted strains above the cavern roofs of the three expansion caverns are less the critical limit of 2.0 millistrain, thus wells to the caverns should not yield. The expansion does not make the structural stability of the existing caverns worse. Finally, the simulations show that from a structural viewpoint, the proposed locations of the two new caverns are acceptable, and the three expansion caverns can be safely constructed and operated.

7 REFERENCES

Ballard, S. and B.L. Ehgartner, 2000. *CAVEMAN Version 3.0: System for SPR Cavern Pressure Analysis,* SAND2000-1751, Sandia National Laboratories, Albuquerque, NM.

Carmichael, R. S., 1984. *CRC Handbook of Physical Properties of Rocks*, CRC (Chemical Rubber Company) Press, Inc. Boca Raton, FL.

Dames and Moore, 1978. *Determination of Physical Properties of Salt and Caprock, Bayou Choctaw Salt Dome, Iberville Parish, Louisiana:* in PB/KKB, Inc., 1978. Salt Dome Geology and Cavern Stability, Bayou Choctaw, Louisiana, Final Report, Appendix, prepared for the U.S. Department of Energy, August 1978.

DOE, 2001. *SPR Level III Design Criteria*, November 2001.

Ehgartner, B.L. and A.S. Lord, 2006. *Draft Specifications for Two New Caverns at Bayou Choctaw*, Memo to Wayne Elias, DOE SPR PMO, FE-4432, Sandia National Laboratories, Albuquerque, New Mexico, January 31, 2006.

Ehgartner, B. L. and S.R. Sobolik, 2002. *3-D cavern Enlargement Analyses*, SAND2002-0526, Sandia National Laboratories, Albuquerque, NM.

Hoffman, E.L., 1992. *Investigation of Analysis Assumptions for SPR Calculations*, memo to J.K. Linn, Sandia National Laboratories, Albuquerque, NM, February 7, 1992.

Hogan, R.G., 1980. *Strategic Petroleum Reserve (SPR) Geological Site Characterization Report Bayou Choctaw Salt Dome*, SAND80-7140, Sandia National Laboratories, Albuquerque, NM.

Krieg, R.D., 1984. *Reference Stratigraphy and Rock Properties for the Waste Isolation Pilot Plant (WIPP) Project*, SAND83-1908, Sandia National Laboratories, Albuquerque, NM.

Morgan, H.S. and R.D. Krieg, 1988. *A Comparison of Unified Creep-Plasticity and Conventional Creep Models for Rock Salt Based on Predictions of Creep Behavior Measured in Several in Situ and Bench-Scale Experiments*, SAND87-1867, Sandia National Laboratories, Albuquerque, NM and Livermore, CA.

Neal, J.T., T.R Magorian, K.O. Byrne, and S. Denzler, 1993. *Strategic Petroleum Reserve (SPR) Additional Geologic Site Characterization Studies Bayou Choctaw Salt Dome, Louisiana*, SAND92-2284, Sandia National Laboratories, Albuquerque, New Mexico 87185, Livermore, California 94550.

Park, B.Y., B.L. Ehgartner, C.G. Herrick, and M.Y. Lee, 2008. Numerical Simulation Evaluating the Structural Stability of the Strategic Petroleum Reserve (SPR) in Bayou Choctaw Salt Dome, USA, *The 42nd U.S. Rock Mechanics Symposium and the 2nd U.S.-Canada Rock Mechanics Symposium, held in San Francisco, CA, June 28-July 3*, 2008., ARMA 08-150.

Park, B.Y., B.L. Ehgartner, and M.Y. Lee, 2006. *Three Dimensional Simulation for Bayou Choctaw Strategic Petroleum Reserve (SPR)*, SAND2006-7589, Sandia National Laboratories, Albuquerque, NM.

Thorton, C.H. and I.P. Lew, 1983. *Concrete and Design Construction*, Standard Handbook for Civil Engineers, Chapter 8, 3rd ed., F.S. Merritt, editor, McGraw-Hill, NY.

URS, 2006. *Billion Barrel Expansion, Bayou Choctaw. Draft Conceptual Design Report*, Report prepared for U.S. DOE (Contract DE-AC96-05PO92421), March 2006.

8 ACKNOWLEDGEMENTS

This research is funded by SPR programs administered by the Office of Fossil Energy (FE) of the U.S. Department of Energy. Sandia is a multi program laboratory operated by Sandia Corporation, a Lockheed Martin Company, for the United States Department of Energy's National Nuclear Security Administration under Contract DE-AC04-94AL85000.